ACS APPLIED MATERIALS & INTERFACES

SPOTLIGHT ON APPLICATIONS

www.acsami.org

Light and Dark-Activated Biocidal Activity of Conjugated Polyelectrolytes

Eunkyung Ji,[†] Thomas S. Corbitt,[†] Anand Parthasarathy,[‡] Kirk S. Schanze,*[,‡] and David G. Whitten*[,†]

[†]Department of Chemical and Nuclear Engineering and Center for Biomedical Engineering, University of New Mexico, Albuquerque, New Mexico 87131-1341, United States

[‡]Department of Chemistry, University of Florida, Gainesville, Florida 32611-7200, United States

ABSTRACT: This Spotlight on Applications provides an overview of a research program that has focused on the development and mechanistic study of cationic conjugated polyelectrolytes (CPEs) that function as light- and dark-active biocidal agents. Investigation has centered on poly-(phenylene ethynylene) (PPE) type conjugated polymers that are functionalized with cationic quaternary ammonium solubilizing groups. These polymers are found to interact strongly with Gram-positive and Gram-negative bacteria, and upon illumination with near-UV and visible light act to rapidly kill the bacteria. Mechanistic studies suggest that the cationic PPE-type polymers efficiently sensitize singlet oxygen ($^1O_2$), and this cytotoxic agent is responsible for initiating the sequence of events that lead to light-activated bacterial killing. Specific CPEs also exhibit dark-active antimicrobial activity, and this is believed to arise due to interactions between the cationic/lipophilic polymers and the negatively charged outer membrane characteristic of Gram-negative bacteria. Specific results are shown where a cationic CPE with a degree of polymerization of 49 exhibits pronounced light-activated killing of *E. coli* when present in the cell suspension at a concentration of 1 μg mL^{-1}.

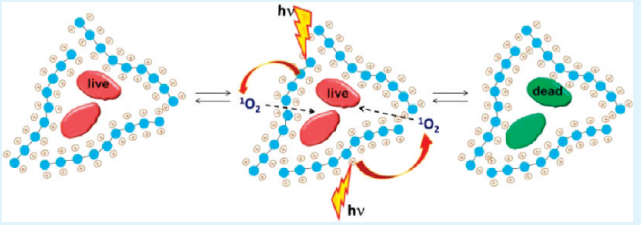

KEYWORDS: conjugated polyelectrolytes, light activated biocides, amplified quenching, singlet oxygen, antibacterial, antimicrobial

INTRODUCTION

Design and development of antimicrobials are of critical importance in various areas such as medical devices, healthcare products, water purification systems, food packaging, food storage and household sanitation, among other applications. Contamination by microorganisms such as bacteria is a major problem in these areas.[1] Furthermore, increasing bacterial resistance to currently available antibiotics has created a serious health crisis; therefore, new antibacterial strategies are required to replace conventional antimicrobial materials. An alternative would be creating biocidal surfaces that could efficiently kill both waterborne and airborne bacteria on contact.[2] These types of bactericidal surfaces have been fabricated by anchoring antimicrobials covalently onto textiles and hard surface of materials such as cottons, glasses, and plastics,[2] and efforts have recently been devoted to linking antimicrobial agents to long and flexible polymers immobilized onto solid surfaces.[3] Several classes of polymeric antimicrobials have been reported including N-halamine polymers,[4−9] poly(4-vinyl-N-alkylpyridium),[10−13] polymeric quaternary ammonium compounds,[14−16] and poly-(N-vinylguanidine).[17]

Interestingly, photodynamic inactivation of microorganisms was first reported more than 100 years ago, but greatly decreased in popularity after discovery of antibiotics.[18,19] However, the release of new antibiotics was immediately followed by the development of resistant strains of bacteria, which have driven research into application of photosensitizers that are successfully used in photodynamic therapy. A large number of antimicrobial photosensitizers, including dyes such as rose bengal and methylene blue, phenothiazines, porphyrins, phthalocyanines, and inorganic semiconductor nanoparticles such as TiO_2 and ZnO, have been tested as antimicrobial agents.[20,21] It is well-established that singlet oxygen ($^1O_2$) plays a key role in photodynamic inactivation of bacteria to induce cell damage or death because this reactive form of oxygen causes degradation of cell walls, lipid membranes, enzymes, and nucleic acids.[22−26] In particular, the cytoplasmic membrane is the crucial target to induce irreversible damage in bacteria after irradiation.[18] When photosensitizers are able to accumulate in significant amounts in or at the cytoplasmic membrane, they show efficient photodynamic inactivation of bacteria. Positively charged photosensitizers show an affinity for these membranes and have been reported as successful antimicrobials.[18]

Tew and co-workers produced examples of conjugated polyelectrolytes (CPEs) with antibacterial activity and selectivity to bacterial or mammalian cells.[27−29] These synthetic polymers based on meta-linked poly-(phenylene ethynylene)s containing polar, cationic, and nonpolar alkyl groups along the backbone mimic the facially amphiphilic structure and biological properties of host defense peptides. It was also demonstrated that activity and selectivity of their polymers were controlled by their nonpolar groups and total molecular weight.[28] This work showed the notable potential of CPEs as antimicrobial agents. However, it is

Received: May 19, 2011
Accepted: June 30, 2011
Published: July 14, 2011

 © 2011 American Chemical Society

Chart 1. Chemical Structures of Some CPEs

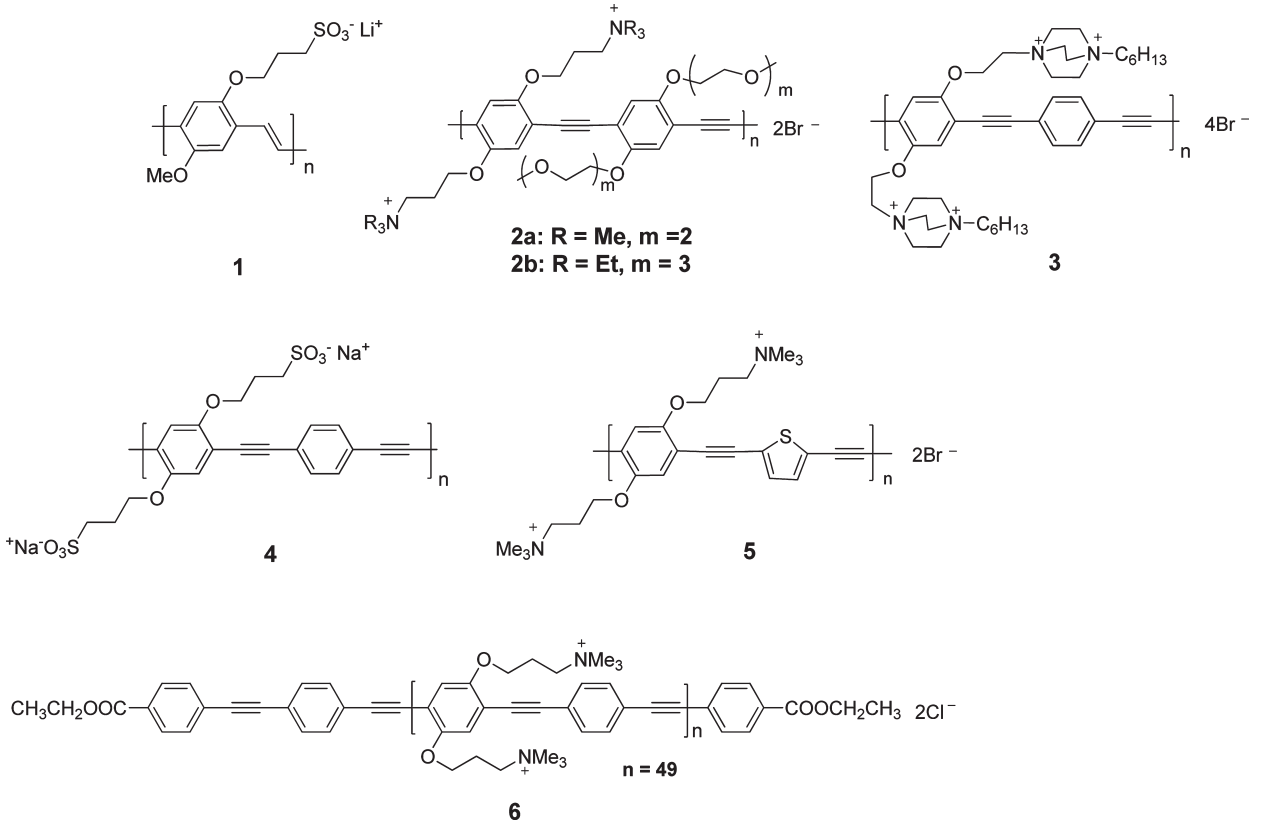

also important to recognize that CPEs have light-harvesting properties; thus they are capable of generating $^1O_2$ or other reactive oxygen species (ROS) to enhance their biocidal activity.

In this Spotlight on Applications, we focus on light and dark-activated biocidal activity of cationic conjugated polyelectrolytes based on linear poly-(phenylene ethynylene) backbones functionalized with tetraalkylammonium functional groups. We describe the early studies demonstrating the light-activated biocidal activity of this class of polymers, along with investigations carried out to understand the mechanism, including photophysical studies of triplet formation and singlet oxygen sensitization. Model membrane studies provide evidence regarding the mechanism of the dark-activated biocidal activity. Finally, we illustrate some recent results obtained using flow cytometry based high throughput screening, which has allowed us to rapidly screen a family of polymers allowing the development of structure−activity relationships for the light- and dark-biocidal activity.

The objective of this Spotlight Article is to highlight work by our group in this area of applied materials research. Some relevant work on related polymeric biocidal materials is reviewed; however, this article is not intended to be a comprehensive review of the field of biocidal polymers. The reader is referred to several comprehensive review articles for a more thorough review of the recent literature regarding biocidal polymers.[1,2,30]

CONJUGATED POLYELECTROLYTES

Conjugated polyelectrolytes (CPEs) are π-conjugated polymers featuring ionic side groups. CPEs contain a π-conjugated backbone such as poly(*p*-phenylene vinylene) (PPV), poly-(*p*-phenylene) (PPP) or poly(*p*-phenylene ethynylene) (PPE), that is further functionalized with pendant ionic functional groups such as sulfonate, carboxylate or tetraalkylammonium.[31] Example chemical structures of CPEs are shown in Chart 1. CPEs exhibit the electronic and optical properties intrinsic to their π-conjugated backbone as well as solubility and hydrophilicity enabled by the addition of charged side chains. A large number of studies of CPEs have focused on their use in chemo- and biosensors because they exhibit the property of "amplified fluorescence quenching" by oppositely charged quencher ions.[31,32] Swager and Zhou[33,34] first demonstrated the concept of amplified quenching in fluorescent conjugated polymers and the first example of amplified quenching in a CPE was reported by Whitten and co-workers.[35] In most CPE-based sensors, fluorescence is either enhanced ("turn-on" approach) or quenched ("turn-off" approach) by interacting with quencher ions or quencher-ligands.[32] The CPE sensors are based on several mechanisms including superquenching of fluorescence, fluorescence resonance energy transfer (FRET), polymer backbone conformation change, or polymer (de)aggregation that is induced by interaction with target analytes. Additionally, CPE films can be produced via layer-by-layer (LBL) self-assembly, which enables the fabrication of thin-film-based optoelectronic devices.[32]

INITIAL STUDIES OF LIGHT-ACTIVATED BIOCIDAL ACTIVITY OF CATIONIC CONJUGATED POLYELECTROLYTES

In initial studies, Whitten and co-workers reported that the cationic *poly*-(phenylene ethynylene)-based CPE **2a** with quaternary

ammonium groups exhibited light activated biocidal activity against Gram-negative bacteria such as *Escherichia coli* (*E. coli*) and Gram-positive bacterial spores such as *Bacillus anthracis* (*B. anthracis*).[36] Incubation of CPE **2a** with *E. coli* or *B. anthracis* spores resulted in coating of both types of bacteria with CPE **2a**, as demonstrated by the fact that the cells exhibit strong fluorescence after treatment (Figure 1). The CPE **2a** coating effectively kills the bacteria upon irradiation with white light. In contrast, there is little or no biocidal activity when the CPE-treated bacteria are illuminated with yellow light. When the bacteria are treated with a solution containing a moderate or high concentration of CPE **2a**, the excess polymer that remains in solution affords protection to the CPE-coated bacteria by the inner filter effect of CPE **2a**, leading to inhibition of the biocidal activity and enhanced bacterial survival (Figure 2).[36]

MECHANISM OF LIGHT-ACTIVATED BIOCIDAL ACTIVITY

During the past several years, we have carried out a variety of studies to investigate the mechanism of the light-activated biocidal activity exhibited by CPEs.[37−41] These investigations have included photophysical probes such as steady state and time-resolved absorption and fluorescence spectroscopy. As outlined below, the studies strongly support a model in which the CPEs serve as efficient sensitizers of singlet molecular oxygen ($^1O_2$). This highly reactive form of oxygen is believed to be the primary biocidal agent, and it is produced by energy transfer from the triplet excited state of the cationic CPEs. Since the CPEs are in close proximity to the bacteria, the $^1O_2$ does not have to diffuse far to elicit its toxic effect on the target microorganism.

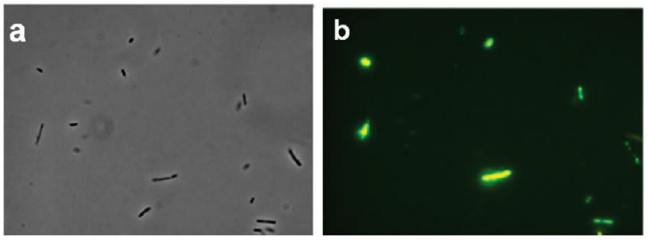

Figure 1. (a) Phase contrast and (b) fluorescence (dark-field) microscope images of E.*coli* after treatment with a dilute solution of **2a**. The green fluorescence seen in the dark-field image arises from the polymer. Reprinted with permission from ref 36. Copyright 2005 ACS Publications.

Transient absorption spectroscopy has been utilized extensively to investigate the triplet states of cationic CPEs.[37,38] Direct excitation of PPE-based conjugated polymers first produces a singlet excited state that undergoes intersystem crossing with moderate efficiency (ϕ_{isc} = 0.05−0.20) to produce a triplet state (triplet exciton). The triplet state is readily detected by transient absorption spectroscopy, in which a long-lived (τ = 5−20 μs) absorption is observed throughout the visible and into the near-infrared region (Figure 3a).[37,38] The triplet of the PPE polymers is sufficiently energetic ($E_T \approx$ 2.0−2.2 eV) such that it is able to undergo energy transfer to ground state triplet dioxygen ($^3O_2$) leading to efficient production of $^1O_2$ (Figure 3b). Evidence that $^1O_2$ is produced is provided by near-infrared photoluminescence spectroscopy carried out with the cationic CPEs in air-saturated CD_3OD solution. Here the emission of the $^1O_2$ that is sensitized by the CPE is readily detected by its characteristic emission at 1260 nm (Figure 3c). Quantum yield experiments indicate that typical cationic CPEs produce $^1O_2$ with yields in the range from 0.01−0.1 in CD_3OD solution.

Because the biocidal experiments are typically carried out in aqueous solution, evidence that $^1O_2$ is produced by cationic CPEs in water was also sought. Because the lifetime of $^1O_2$ is considerably shorter in water than in CD_3OD, it is not possible to directly observe it via near-infrared photoluminescence. In this case, we turned to the use of a chemical agent which is able to trap even short-lived $^1O_2$ by a very rapid bimolecular cycloaddition reaction. These experiments were carried out using the water-soluble chemical trap 1,3-cyclohexadiene-1,4-diethanoate (CHDDE), which forms a stable endoperoxide when it reacts with $^1O_2$. In these experiments disappearance of CHDDE was monitored by decrease of its absorption at 270 nm as a function

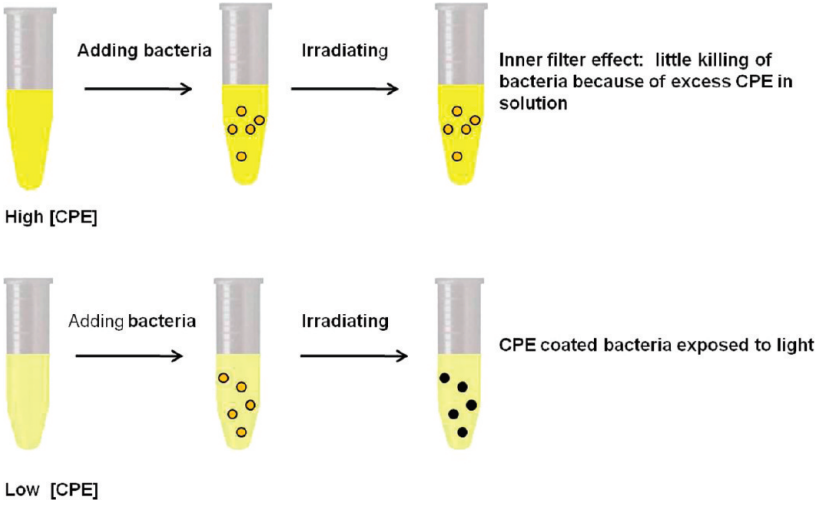

Figure 2. Schematic representation of inner filter effect of biocidal CPE in solution. Top row shows the effect of treatment of bacteria with a solution containing a high concentration of CPE. CPE coats the bacteria, but the polymer that remains in solution acts to filter the incident light leading to little bacteria killing. The bottom row shows the effect of treatment of bacteria with a solution containing a low concentration of CPE. In this case, the incident light reaches the coated bacteria leading to efficient light-activated killing. The interested reader is directed to ref 36 for details concerning the conditions for these experiments.

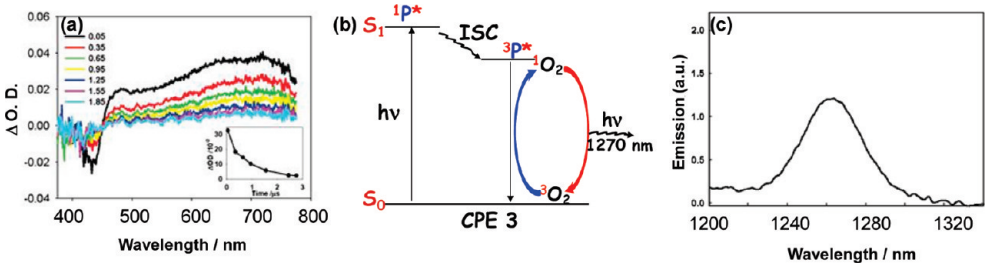

Figure 3. (a) Transient absorption difference spectra of CPE **3** in methanol, (b) schematic representation for the formation of singlet oxygen sensitized by CPE, and (c) singlet oxygen emission at $\lambda \approx 1260$ nm sensitized by CPE **3** in CD_3OD. Reprinted with permission from ref 38. Copyright 2009 Royal Society of Chemistry Publishing.

Scheme 1. General mechanism of biocidal action by CPEs: (a) Reversible bacterial adhesion on to CPE chains; (b) Light absorption by CPE to generate singlet oxygen, which subsequently attacks live bacteria; and (c) Killed bacteria adhere to CPE chains[a]

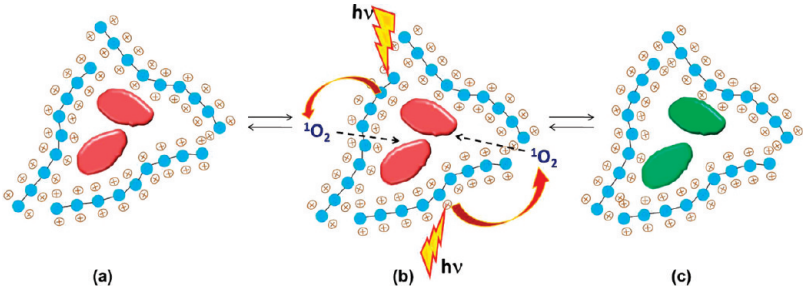

[a] live bacteria shown in red and dead bacteria shown in green.

Scheme 2. Synthesis of silica particles that contain surface-grafted PPE-type conjugated polyelectrolyte. Reprinted with permission from ref 46. Copyright 2007 ACS publications.

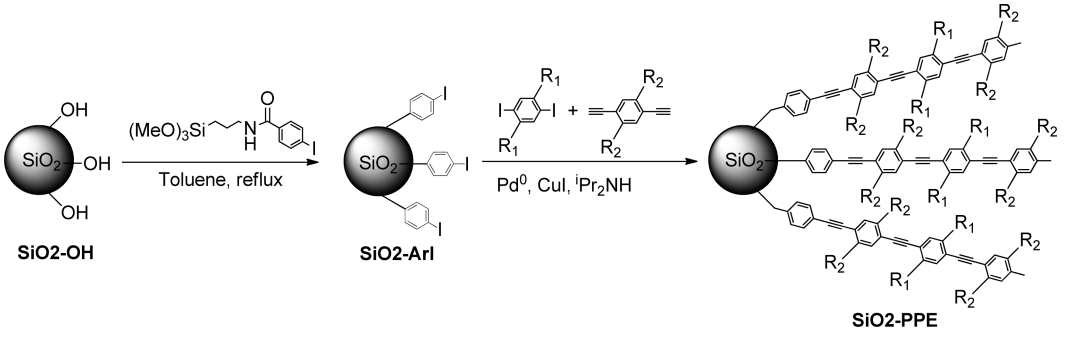

of irradiation time in aqueous solution with cationic CPEs **2a**, **3**, and **5**.

The above results clearly demonstrate that $^1O_2$ can be efficiently generated by irradiating cationic CPEs. It has been well established that singlet oxygen and other reactive oxygen species (ROS) induce severe damage or death to microorganisms.[42−45] Taken together, the photophysical and photochemical studies suggest the plausibility of light-activated biocidal action that is outlined in Scheme 1.[37] First, the solution borne CPE adsorbs to the surface of the bacteria, with possible interaction between the cationic side groups and the negatively charged bacterial membrane (a). Second, $^1O_2$ is produced at the polymer/bacteria interface during irradiation of the polymer (b). The singlet oxygen or subsequently produced reactive oxygen intermediates interact with the bacteria resulting in bacteria death (c).

LIGHT-ACTIVATED BIOCIDAL ACTIVITY OF CPE-GRAFTED PARTICLES AND POLYELECTROLYTE CAPSULES

We have also prepared and characterized anionic conjugated polyelectrolyte-grafted silica particles.[46] The surface of the silica microspheres was modified with silane functionalized iodobenzene and the Sonogashira polymerization of a 1,4-diiodobenzene and 1,4-diethynylbenzene was performed in solution containing the functionalized silica particles (Scheme 2). The polymerization reaction afforded silica particles that contain a surface-grafted layer of a cationic poly(phenylene ethynylene)-based CPE. The resulting surface-grafted particles exhibit strong fluorescence from the CPE that is covalently bonded to the silica surface. The surface grafted conjugated polymer (SGCP) has the

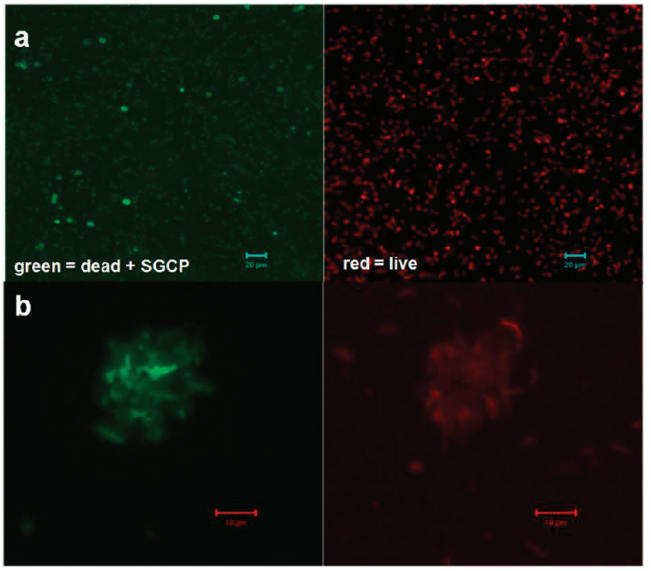

Figure 4. Composite confocal microscope images of CPE **2b**-surface grafted silica beads (5 μm) **SGCP-2b** with *C. marina* after irradiation for 15 min in ambient air. Left column of images shows green channel which corresponds to dead bacteria and fluorescence from the CPE-grafted particles (SGCP). Right column shows red channel which corresponds to live bacteria. Top row (a) shows large field of view (20 μm scale bar) and bottom row (b) shows increased magnification view (10 μm scale bar) with field focused on a single cluster of SGCPs with bacteria (mainly dead). Reprinted with permission from ref 37. Copyright 2008 ACS Publications.

advantage of acting as a biocide on a solid surface; it is reusable after washing and prevents uncontrolled release of the polymer material into the environment.

Because CPE **2a** was shown to exhibit light-induced biocidal effect,[36] the structurally similar cationic CPE **2b** was grafted to the surface of silica particles by the procedure in Scheme 2.[37] The light-activated biocidal activity of CPE **2b** grafted particles was investigated against two Gram negative bacteria: *Cobetia marina* (*C. marina*) and *Pseudomonas aeruginosa* strain PAO1 (*P. aeruginosa*). These experiments were carried out using confocal microscopy combined with live/dead fluorescent dye stains to assess the viability of the bacteria exposed to light or maintained in the dark (control). For the light-exposed suspension of CPE **2b**-coated particles and bacteria, bacteria that are associated with or in the vicinity of the particles were effectively killed in solution exposed to ambient air (Figure 4). As shown in the close up image (Figure 4b), clusters of particles and bacteria build up during the irradiation; note that most of bacteria in the cluster are dead as green fluorescence from the dye (SYTOX Green) is dominant in the confocal fluorescence image. Counting assays were performed from the confocal fluorescence images to quantify the dead/live ratio under various conditions.[37] The light-exposed SGCP/bacteria suspension in ambient air exhibited a small increase in the number of dead bacteria compared to suspension kept in the dark as a control. However, when the suspension was purged with oxygen and irradiated with visible light a substantial increase in the dead/live ratio was seen compared to the control. In contrast, deoxygenated suspensions exhibit low dead/live ratio both in dark and when irradiated. This observation clearly supports the proposed role of singlet oxygen in the biocidal activity.

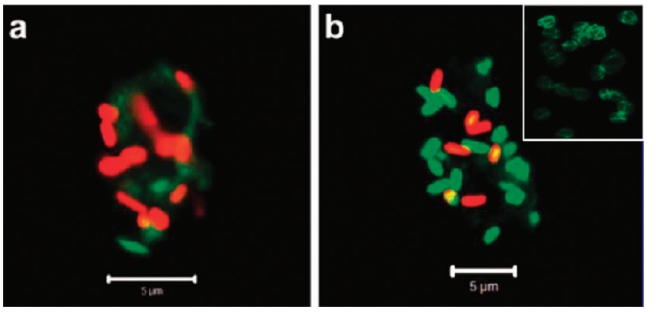

Figure 5. Composite confocal microscope images of polyelectrolyte capsules consisting of four bilayers of CPEs **3** and **4** (μRMs) with trapped *P. aeruginosa* bacteria (a) before and (b) after 15 min of irradiation with white light from a fiber lamp. The live/dead stain set used indicates red = live and green = dead. The CPE capsule can be seen as a faint green circle in part (a), and it is barely discernible as green emission in the lower region of the cluster in part (b). The inset shown in part (b) is an epifluorescence image of the CPE capsules prior to mixing with the bacteria. The scale bars in the confocal images are 5 μm, and the approximate size of the capsules in the epifluorescence image in the inset is 5 μm diameter. Reprinted with permission from ref 39. Copyright 2009 ACS Publications.

More recently, we reported the preparation of CPE microcapsules consisting of alternating layers of oppositely charged CPEs, which are referred to as "micro Roach Motels" (μRMs).[39] The CPE microcapsules are fabricated by layer-by-layer (LbL)[3,47−50] deposition of four bilayers consisting of anionic CPE **3** alternating with cationic CPE **4** supported on 5 μm-diameter $MnCO_3$ template particles. Following the LbL deposition sequence, the $MnCO_3$ template is dissolved by using a solution of ethylenediaminetetraacetate (EDTA); the resulting hollow capsules are approximately 5 μm in diameter and they exhibit the strong green fluorescence characteristic of the PPE-type polymers **3** and **4** (see inset in Figure 5b). The antimicrobial activity of the CPE based capsules (μRM) against *P. aeruginosa* and *C. marina* was monitored by confocal fluorescence microscopy by staining the bacteria with a 1:1 mixture of SYTO 60 (red emission = live) and SYTOX Green (green emission = dead) stains (see Figure 5). As shown in Figure 5a, the μRMs very effectively able to capture bacteria, forming clusters consisting of bacteria ensnared by the μRMs. After exposing the suspension containing the bacteria and μRMs to visible light for 15 min, most of the bacteria associated with the μRMs are dead, as evidenced by the green fluorescence emission characteristic of the dead stain (Figure 5b). The experiments demonstrate that the CPE based micro Roach Motels are particularly effective at capturing and killing bacteria in suspension.

DARK BIOCIDAL ACTIVITY OF CATIONIC CONJUGATED POLYELECTROLYTES

During our studies of the light-activated biocidal activity of cationic CPEs, we discovered that CPE **5**, which contains a 2,5-thienylene repeat unit within the conjugated polymer backbone was unlike other CPEs that had been investigated. Specifically, CPE **5** was found to exhibit significant dark biocidal activity against *P. aeruginosa*, but little light-activated activity.[38,51] As illustrated in Figure 6a, when a suspension of glass microspheres coated with a physisorbed layer of CPE **5** is mixed with *P. aeruginosa* in the dark the microspheres and bacteria begin

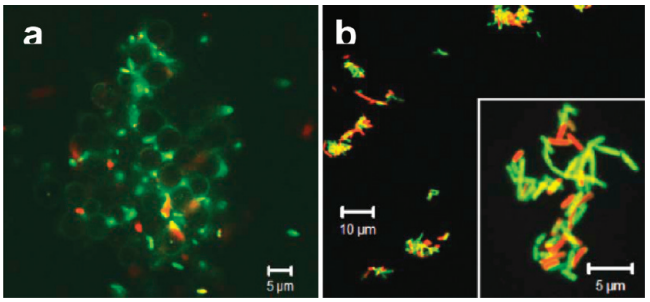

Figure 6. Confocal microscope images of *P. aeruginosa* strain PAO 1 bacteria added to a suspension of 5 μm diameter glass microspheres coated with (a) a layer of physisorbed polymer **5** and (b) a solution of polymer **5**. In both cases, the bacteria/polymer suspensions were kept in the dark. In the images red-stained bacteria are live, and green-stained bacteria are dead. The yellow color indicates bacteria that have been compromised and exhibit both red and green emission. Scale bars: (a) 5 and (b) 10 μm. Reproduced from ref 38 by permission of the Royal Society of Chemistry (RSC) for the European Society for Photobiology, the European Photochemistry Association, and the RSC.

to form large clusters and concurrently the bacteria are killed.[38] Cluster formation is attributed to release of microbial agglutinants as the cell membranes are damaged by contact with the CPE-coated microspheres. When *P. aeruginosa* is mixed with CPE **5** in solution in the dark, clusters of bacteria are again seen to form, and the bacteria are rapidly killed, Figure 6b. The unique dark biocidal activity of CPE **5** and its ability to induce aggregation/clustering of the bacteria is believed to arise from the polymer's significant lipophilic character. The lipophilicity of polymer **5** was demonstrated by the observation of a dramatic enhancement of the polymer's fluorescence when liposomes of the anionic phospholipid 1,2-dioleoyl-*sn*-glycero-3-[phospho-rac-(1-glycerol)] (sodium salt) (DOPG) were added to an aqueous solution of the polymer.[38] The increased fluorescence is attributed to the dissociation of polymer aggregates induced by a "dissolving" of the polymer into the DOPG liposome via hydrophobic and electrostatic interactions between the polymer and the phospholipid bilayer.

Further investigation into the interactions of cationic CPEs with lipid membranes was carried out to understand the dark biocidal mechanism and to assess structure−activity relationships for the biocidal activity. Anionic phosphatidylglycerol (PG) model membrane systems were used for this investigation in order to mimic the bacteria cell membrane. The systems investigated included PG liposomes in aqueous solution and PG lipid monolayers at the air−water interface.[52,53] Interaction of CPE **5** with lipid membranes were assessed by monitoring changes in the fluorescence spectra of the polymer, increase of the monolayer surface area or pressure upon addition of the polymer to the subphase, and changes in liposome size. A fluorescent rhodamine dye-labeled phospholipid, 1,2-dimyristoyl-*sn*-glycero-3-phosphoethanolamine-N-(lissamine rhodamine B sulfonyl) (ammonium salt) (DMPE-Rh) was incorporated into DOPG liposomes at mole percentages of 0.1−1 to provide information about the distance between the CPE **5** and the liposome using fluorescence energy transfer (FRET) which reports on interactions at distances in the range of 1−10 nm. It was found that excitation of CPE **5** with light absorbed primarily by the polymer resulted in quenching of the fluorescence from CPE **5** and sensitization of the fluorescence of DMPE-Rh, confirming the close proximity of the polymer to the

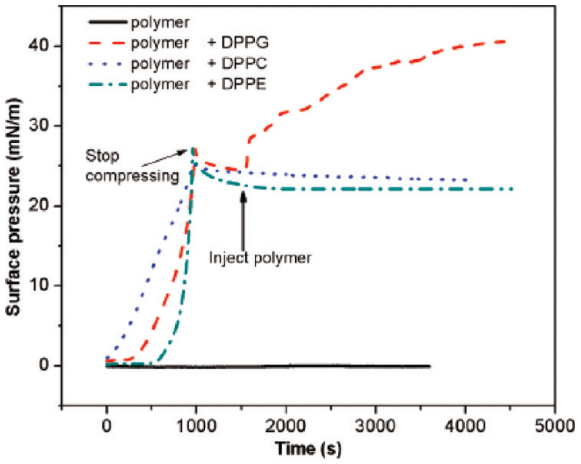

Figure 7. Monitoring monolayer films at the air−water interface formed by spreading and then compressing pure phospholipids. The red dashed line monitors the surface pressure of a film of anionic DPPG, the green dashed line shows the surface pressure of a film of zwitterionic DPPE and the black dotted line shows the surface pressure of a film of zwitterionic DPPC. The solid black line indicates that CPE **5** by itself does not form a film at the air−water interface. The films are compressed to 25 mN/m and then, in each case, an aliquot of aqueous CPE **5** is injected into the subphase beneath the film. For the film from anionic DPPG there is an increase in surface pressure following the addition of CPE **5** indicating the polymer is being incorporated into the film. The lack of increase in surface pressure following polymer addition beneath the film suggests there is little interaction between CPE **5** and the films from the neutral (zwitterionic) phospholipids. Reprinted with permission from ref 53. Copyright 2010 ACS Publications.

fluorescently labeled lipid.[52] It also has been observed that the CPE **5**-liposome mixture exhibits suppressed fluorescence quenching by 9,10-anthraquinone-2,6-disulfonic acid disodium salt (AQS) compared to polymer alone.[52] These results support the notion that cationic CPE **5** first associates with the anionic lipid membrane via electrostatic interactions and then inserts into the bacterial membrane interior due to the hydrophobic interactions between the polymer and the lipid membrane. Once CPE **5** is incorporated or entrapped within the membrane, there is some alteration of the packing and organization of the lipids, which could affect membrane permeability and thus give rise to the polymers' dark biocidal activity.

Addition of CPE **5** to lipid monolayers and liposomes formed from anionic phospholipids causes an increase in the monolayer surface area or pressure, and liposome size, respectively.[52,53] These observations also confirm the strong interactions between the CPE **5** and certain lipid membranes. An interesting question is that of possible selectivity of antimicrobials when their reactivity is assessed against phospholipid membranes of different charge and composition: bacterial membranes are usually an excess of negatively charged phospholipids and an overall negative charge, while mammalian membranes are predominantly zwitterionic with little net charge on their surfaces.[54] Therefore, anionic PG lipid membranes and zwitterionic phosphatidylcholine (PC) and phosphatidylethanolamine (PE) lipid membranes were compared to evaluate the potential membrane selectivity of CPE **5**.[53] The polymer was injected into the aqueous subphase of monolayer films at the air−water interface of 1,2-dipalmitoyl-*sn*-glycero-3-[phospho-rac-(1-glycerol)] (DPPG), 1,2-dipalmitoyl-*sn*-glycero-3-phosphatidylcholine (DPPC),

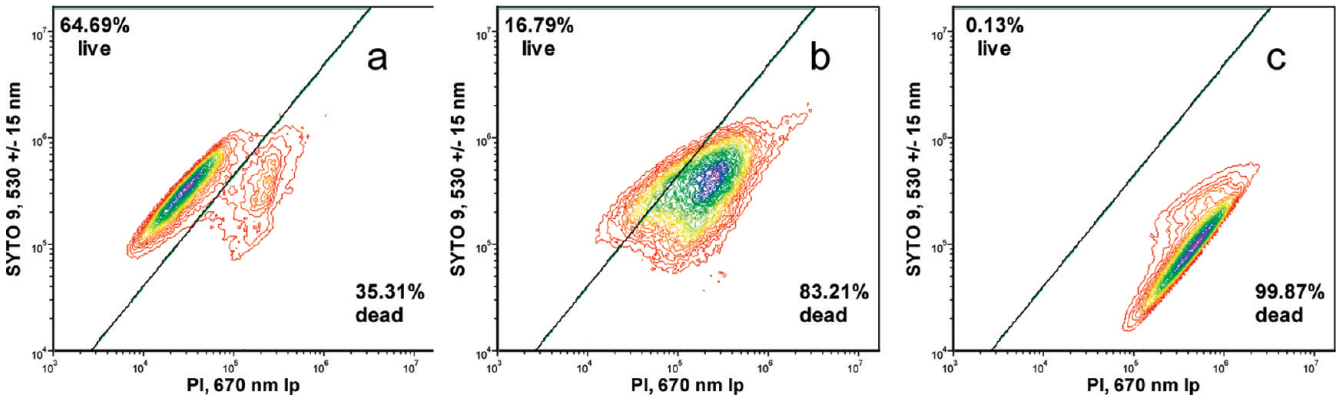

Figure 8. Evolution of an *E. coli* population over time upon exposure to CPE **6** (n = 49, 1 μg mL^{-1}) in near-UV light (365 nm). Measurements were taken at (a) 30, (b) 60, and (c) 120 min using the flow cytometric method. For each plot, the y- and x-axes show counts in the emission channel at 530 nm (green) and >670 nm (red), respectively. The scales are logarithmic and span the range 1 × 10^3 to 1 × 10^7 counts (x-axis) and 1 × 10^4 to 1 ×10^7 counts (y-axis).

and 1,2-dipalmitoyl-*sn*-glycero-3-phosphatidylethanolamine (DPPE). These films had been first compressed to a target pressure of 25 mN/m and then the change of surface pressure following injection of the polymer was monitored. As shown in Figure 7, injection of the polymer under the negatively charged DPPG monolayer immediately induces an increase in the monolayer's surface pressure; however, there are no changes in surface pressure from either the zwitterionic DPPE or DPPC monolayer films. This result suggests that CPE **5** may exhibit an ability to selectively target bacterial cells over mammalian cells due to its strong affinity toward anionic PG lipids.

APPLICATION OF FLOW CYTOMETRY FOR SCREENING BIOCIDAL ACTIVITY

In very recent work, we have developed flow cytometry as a method to rapidly quantify biocidal activity as a function of the CPE structure and concentration in solution. The live/dead stains established for use in confocal microscopy have been used to differentiate live and dead bacterial populations in the flow cytometry setup.[40,55] Data generated by using this technique are relatively easily classified according to live and dead populations, with appropriate consideration given to any potential intermediate populations. In addition, it is possible to rapidly screen in excess of 1 × 10^6 individual bacteria from a given sample, allowing the assessment of the log kill rate with statistical certainty over 6 decades. Examples of the data gathered in a typical flow cytometry experiment are shown in Figure 8, where the evolution of a population of *E. coli* when mixed in suspension with CPE **6** (1 μg mL^{-1}) is monitored. The contour plots in Figure 8 show counts in the green channel (y-axis, 530 nm, live stain) vs counts in the red channel (x-axis, 670 nm, dead stain). In this particular presentation, it can be seen that the population evolves from exhibiting a large number of counts in the green channel (~64.7% live) to the predominant number of counts in the red channel (~99.9% dead).

A summary of a more extensive set of experiments for biocidal activity of CPE **6** that were obtained from flow cytometry analysis is shown below in Figure 9. Here it is seen that the fraction of live bacteria decreases substantially with increasing photolysis time, and that the biocidal effect of the polymer is greater when it is present at 10 μg mL^{-1} compared to 1 μg-mL^{-1}. However, for both concentrations of CPE **6** >99% kill is observed following

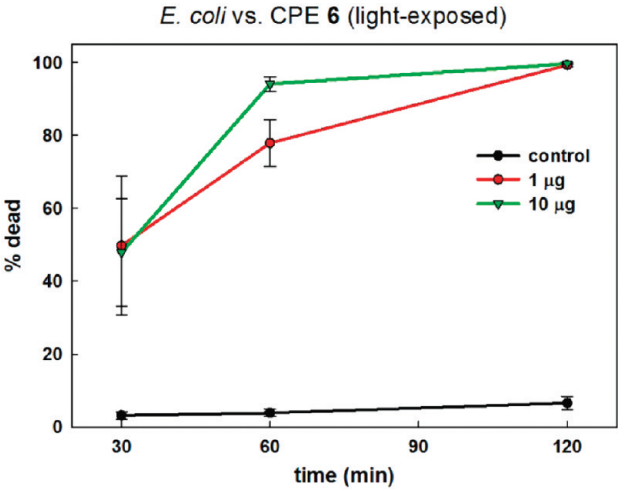

Figure 9. Results of *E. coli* exposure to CPE **6** (n = 49) and to near-UV light (365 nm) at two concentrations (1 and 10 μg/mL). Measurements were taken at 30, 60, and 120 min using the flow cytometric method.

120 min of light exposure. A dark control experiment run in parallel with the light exposed samples shows that CPE **6** exhibits little dark biocidal activity.

To cross-validate the flow cytometry results, parallel experiments are carried out using confocal microscopy to visualize the bacteria with the live/dead stains. As shown in Figure 10, the *E. coli* exhibit bright green (live) fluorescence at the beginning of the experiment (control). However, after a period of light exposure with CPE **6** the bacteria exhibit the yellow-red fluorescence characteristic of the propidium iodide dye, which signals that the membrane of the cells has been damaged by the light-activated action of the polymer.

BIOCIDAL ACTIVITY OF CATIONIC ARYLENE ETHYNYLENE OLIGOMERS

The biocidal studies have been extended to include small molecule oligomer analogs of the PPE-type conjugated polyelectrolytes. This work has allowed us to gain more insight into the relationship between molecular structure, photophysics and the light induced biocidal activity. In addition, this work has led to

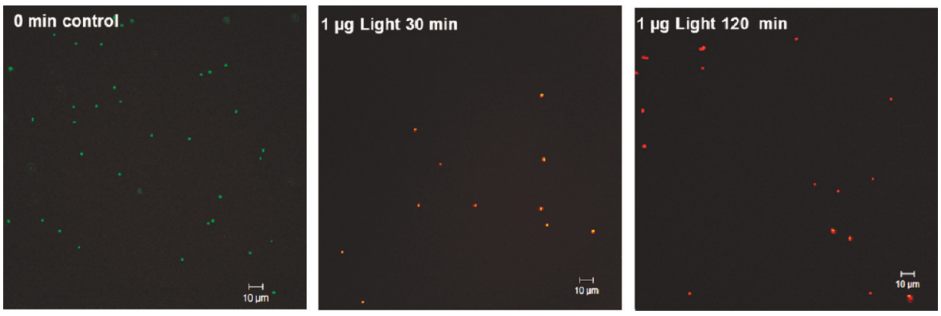

Figure 10. Fluorescence confocal microcopy images of 0 min control (*E.coli* suspension without the polymer) and 30 and 120 min near-UV light-exposed polymer (CPE **6** (n = 49), 1 μg/mL) /*E.coli* suspension, respectively. Green fluorescent (SYTO 9) cells represent live cells, whereas red fluorescent (propidium iodide) cells represent dead or compromised cells.

Chart 2. Chemical Structures of OPEs

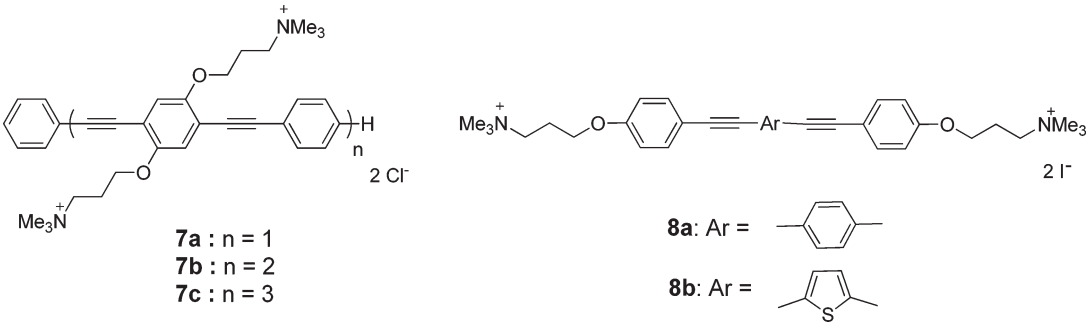

development of specific molecular compounds that are particularly active light-activated antimicrobials. Here we summarize some of the most significant findings of this work, and the reader is directed to the primary literature for details.[40,41]

In one line of investigation, we prepared the series of cationic oligo-(phenylene ethynylene)s (OPEs) **7a**−**c** (Chart 2) in order to examine the relationship between conjugation length, photophysics, and biocidal activity. The structures of these OPEs are similar to those of the CPEs shown in Chart 1, where the cationic tetraalkylammonium groups are appended as "side groups" to alternating repeat units in the conjugated chain. As described above, in photophysical experiments we probe the relative triplet and $^1O_2$ yields, and then this data is correlated with the light-activated biocidal activity. Interestingly for series **7a**−**c** a clear trend emerges. In particular, it is seen that the relative triplet yield decreases as the oligomer length increases (e.g., **7a** > **7b** > **7c**), and at the same time the sensitized yield of $^1O_2$ varies in the same order. Although this series of OPEs displays only weak dark biocidal activity, each of the oligomers exhibits relatively strong light-activated biocidal activity against the Gram-positive bacteria *S. aureus*. The most interesting result of this study is the fact that the light-activated biocidal activity varies as predicted by the photophysical data. Specifically, the light-activated biocidal activity of the series varies in the order **7a** > **7b** > **7c**, which supports the premise that the light-activated biocidal activity is correlated with the ability of the oligomer to sensitize $^1O_2$. In addition, this study reveals that the shortest oligomer **7a** is a comparatively effective biocide against Gram-positive bacteria, exhibiting high activity (>log 2 to log 3 killing rate) with 30−60 min of light exposure when present at a concentration of 50 ng mL^{-1}.

In another line of investigation, we have explored oligomers in which the quaternary alkylammonium units are attached at the "ends" of the oligomers, **8a** and **8b**, Chart 2. Model membrane studies show that these oligomers are particularly effective at interacting with negatively charged membrane lipid assemblies, possibly because of their linear structures.[56] These end-functionalized oligomers have also been found to be particularly effective light-activated biocides, and the biocidal activity varies as expected on the basis of the photophysical properties. In particular, **8b** exhibits a substantially larger triplet and $^1O_2$ yield compared to **8a**. The difference is attributed to the effect of the 2,5-thienylene ring in **8b** which enhances the rate of intersystem crossing to the triplet manifold. Both of these oligomers are potent light-activated biocides, exhibiting substantial activity at concentrations below 1 μg mL^{-1} in solution against *E. coli*. However, in accord with the photophysical results, oligomer **8b** is substantially more active than **8a**. For example at a concentration of 0.1 μg-mL^{-1} with 60 min light exposure oligomer **8b** exhibits 97.5% kill vs *E. coli* (∼ log 2 reduction) while under the same conditions **8a** achieves only 20% kill. Nonetheless, at higher concentration (1 μg mL^{-1}) both oligomers achieve ∼log 2 kill efficacy vs *E. coli* following 60 min of light exposure.

■ OUTLOOK AND FUTURE DIRECTIONS

This Spotlight on Applications highlights recent work demonstrating the utility of cationic conjugated polymers as light- and dark-activated biocidal agents against a broad spectrum of bacteria. The mechanistic work indicates that the biocidal activity can be traced to two specific features characteristic of these

materials. First, the cationic quaternary ammonium functionality and lipophilic character of the polymers enables them to interact strongly with the bacteria, presumably via association of the cationic groups with the anionic phospholipid membrane that is characteristic of Gram-negative bacteria. In some cases, the CPE-bacterial interaction apparently leads to membrane disruption, which is the fundamental step in the dark-activated biocidal activity. Second, photophysical studies reveal that PPE-type conjugated polymers and oligomers are able to efficiently sensitize formation of singlet oxygen when illuminated with near-UV and/or visible light in the blue region of the spectrum. Singlet oxygen is a known cytotoxic agent, and it is believed to be the key factor in the mechanism of the light-activated biocidal activity. In support of this premise, our investigations reveal a correlation between the efficiency of the CPEs to sensitize singlet oxygen and their light-activated biocidal efficacy.

A key advantage of these polymer based antimicrobial agents is the ability to use organic, polymer and materials chemistry methods to vary the structure and properties of the polymers and tailor them for a specific application. For example, the specific structure and placement of the cationic functional groups can be varied, as well as the structure and band gap of the conjugated polymer backbone. The former leads to differences in the polymers' hydrophilic/lipophilic balance, whereas the latter controls their light absorption properties, triplet yield and their singlet oxygen generation efficiency. In addition, synthesis can be used to incorporate the polymers into a variety of formats, including coatings on hard surfaces and fibers. This provides a powerful ability to use the polymers in a variety of formats for applications such as antibacterial surfaces, coated antibacterial membranes for air or water filtration, and for the fabrication of textiles that are impregnated with light-activated antibacterial agents. These and other applications are the target of our ongoing work on light- and dark-biocidal conjugated polyelectrolytes.

AUTHOR INFORMATION

Corresponding Author

*E-mail: whitten@unm.edu (D.W.); kschanze@chem.ufl.edu (K.S.) TEL: 505-277-5736 (D.W.); 352-392-9133 (K.S.). FAX: 505-277-1292 (D.W.); 352-846-0296 (K.S.).

ACKNOWLEDGMENT

We thank the Defense Threat Reduction Agency for the support of this research through Grant W911NF-07-1-0079. Confocal images were obtained using the confocal laser scanning microscope housed in the W. M. Keck Confocal Microscopy Facility of the UNM Keck Nanofluidics Laboratory.

REFERENCES

(1) Kenawy, E. R.; Worley, S. D.; Broughton, R. *Biomacromolecules* **2007**, *8*, 1359–1384.
(2) Lewis, K.; Klibanov, A. M. *Trends Biotechnol.* **2005**, *23*, 343–348.
(3) Lichter, J. A.; Van Vliet, K. J.; Rubner, M. F. *Macromolecules* **2009**, *42*, 8573–8586.
(4) Worley, S. D.; Sun, G. *Trends Polym. Sci.* **1996**, *4*, 364–370.
(5) Sun, G.; Wheatley, W. B.; Worley, S. D. *Ind. Eng. Chem. Res.* **1994**, *33*, 168–170.
(6) Sun, G.; Chen, T. Y.; Worley, S. D. *Polymer* **1996**, *37*, 3753–3756.
(7) Liang, J.; Owens, J. R.; Huang, T. S.; Worley, S. D. *J. Appl. Polym. Sci.* **2006**, *101*, 3448–3454.
(8) Liang, J.; Chen, Y.; Barnes, K.; Wu, R.; Worley, S. D.; Huang, T. S. *Biomaterials* **2006**, *27*, 2495–2501.
(9) Chen, Y.; Worley, S. D.; Huang, T. S.; Weese, J.; Kim, J.; Wei, C. I.; Williams, J. F. *J. Appl. Polym. Sci.* **2004**, *92*, 363–367.
(10) Lin, J.; Tiller, J. C.; Lee, S. B.; Lewis, K.; Klibanov, A. M. *Biotechnol. Lett.* **2002**, *24*, 801–805.
(11) Milovic, N. M.; Wang, J.; Lewis, K.; Klibanov, A. M. *Biotechnol. Bioeng.* **2005**, *90*, 715–722.
(12) Tiller, J. C.; Lee, S. B.; Lewis, K.; Klibanov, A. M. *Biotechnol. Bioeng.* **2002**, *79*, 465–471.
(13) Tiller, J. C.; Liao, C. J.; Lewis, K.; Klibanov, A. M. *Proc. Natl. Acad. Sci. U. S. A.* **2001**, *98*, 5981–5985.
(14) Huang, J. Y.; Koepsel, R. R.; Murata, H.; Wu, W.; Lee, S. B.; Kowalewski, T.; Russell, A. J.; Matyjaszewski, K. *Langmuir* **2008**, *24*, 6785–6795.
(15) Lee, S. B.; Koepsel, R. R.; Morley, S. W.; Matyjaszewski, K.; Sun, Y. J.; Russell, A. J. *Biomacromolecules* **2004**, *5*, 877–882.
(16) Murata, H.; Koepsel, R. R.; Matyjaszewski, K.; Russell, A. J. *Biomaterials* **2007**, *28*, 4870–4879.
(17) Bromberg, L.; Hatton, T. A. *Polymer* **2007**, *48*, 7490–7498.
(18) Maisch, T.; Szeimies, R. M.; Jori, G.; Abels, C. *Photochem. Photobiol. Sci.* **2004**, *3*, 907–917.
(19) Raab, O. *Z. Biol.* **1900**, *39*, 524–546.
(20) Zerdin, K.; Horsham, M. A.; Durham, R.; Wormell, P.; Scully, A. D. *React. Funct. Polym.* **2009**, *69*, 821–827.
(21) Tegos, G. P.; Hamblin, M. R. *Antimicrob. Agents Chemother.* **2006**, *50*, 196–203.
(22) Kilger, R.; Maier, M.; Szeimies, R. M.; Baumler, W. *Chem. Phys. Lett.* **2001**, *343*, 543–548.
(23) Jones, R. M.; Bergstedt, T. S.; McBranch, D. W.; Whitten, D. G. *J. Am. Chem. Soc.* **2001**, *123*, 6726–6727.
(24) Jones, L. R.; Grossweiner, L. I. *J. Photochem. Photobiol., B* **1994**, *26*, 249–256.
(25) Halliwell, B.; Gutteridge, J. M. C. *Lancet* **1984**, *1*, 1396–1397.
(26) Foote, C. S. *Photochem. Photobiol.* **1991**, *54*, 659–659.
(27) Arnt, L.; Tew, G. N. *Langmuir* **2003**, *19*, 2404–2408.
(28) Arnt, L.; Tew, G. N. *J. Am. Chem. Soc.* **2002**, *124*, 7664–7665.
(29) Arnt, L.; Nusslein, K.; Tew, G. N. *J. Polym. Sci., Part A: Polym. Chem.* **2004**, *42*, 3860–3864.
(30) Timofeeva, L.; Kleshcheva, N. *Appl. Microbiol. Biotechnol.* **2011**, *89*, 475–492.
(31) Thomas, S. W.; Joly, G. D.; Swager, T. M. *Chem. Rev.* **2007**, *107*, 1339–1386.
(32) Jiang, H.; Taranekar, P.; Reynolds, J. R.; Schanze, K. S. *Angew. Chem., Int. Ed.* **2009**, *48*, 4300–4316.
(33) Zhou, Q.; Swager, T. M. *J. Am. Chem. Soc.* **1995**, *117*, 7017–7018.
(34) Zhou, Q.; Swager, T. M. *J. Am. Chem. Soc.* **1995**, *117*, 12593–12602.
(35) Chen, L. H.; McBranch, D. W.; Wang, H. L.; Helgeson, R.; Wudl, F.; Whitten, D. G. *Proc. Natl. Acad. Sci. U.S.A.* **1999**, *96*, 12287–12292.
(36) Lu, L. D.; Rininsland, F. H.; Wittenburg, S. K.; Achyuthan, K. E.; McBranch, D. W.; Whitten, D. G. *Langmuir* **2005**, *21*, 10154–10159.
(37) Chemburu, S.; Corbitt, T. S.; Ista, L. K.; Ji, E.; Fulghum, J.; Lopez, G. P.; Ogawa, K.; Schanze, K. S.; Whitten, D. G. *Langmuir* **2008**, *24*, 11053–11062.
(38) Corbitt, T. S.; Ding, L. P.; Ji, E. Y.; Ista, L. K.; Ogawa, K.; Lopez, G. P.; Schanze, K. S.; Whitten, D. G. *Photochem. Photobiol. Sci.* **2009**, *8*, 998–1005.
(39) Corbitt, T. S.; Sommer, J. R.; Chemburu, S.; Ogawa, K.; Ista, L. K.; Lopez, G. P.; Whitten, D. G.; Schanze, K. S. *ACS Appl. Mater. Interfaces* **2009**, *1*, 48–52.
(40) Zhou, Z. J.; Corbitt, T. S.; Parthasarathy, A.; Tang, Y. L.; Ista, L. F.; Schanze, K. S.; Whitten, D. G. *J Phys Chem Lett* **2010**, *1*, 3207–3212.

(41) Tang, Y. L.; Corbitt, T. S.; Parthasarathy, A.; Zhou, Z. J.; Schanze, K. S.; Whitten, D. G. *Langmuir* **2011**, *47*, 4956–1962.
(42) Lamberts, J. J. M.; Schumacher, D. R.; Neckers, D. C. *J. Am. Chem. Soc.* **1984**, *106*, 5879–5883.
(43) Tzeng, D. D.; Lee, M. H.; Chung, K. R.; Devay, J. E. *Can. J. Microbiol.* **1990**, *36*, 500–506.
(44) Comini, L. R.; Nunez Montoya, S. C.; Paez, P. L.; Argueello, G. A.; Albesa, I.; Cabrera, J. L. *J. Photochem. Photobiol., B* **2011**, *102*, 108–114.
(45) Vargas, F.; Zoltan, T.; Rivas, C.; Ramirez, A.; Cordero, T.; Diaz, Y.; Izzo, C.; Cardenas, Y. M.; Lopez, V.; Gomez, L.; Ortega, J.; Fuentes, A. *J. Photochem. Photobiol., B* **2008**, *92*, 83–90.
(46) Ogawa, K.; Chemburu, S.; Lopez, G. P.; Whitten, D. G.; Schanze, K. S. *Langmuir* **2007**, *23*, 4541–4548.
(47) Antipov, A. A.; Shchukin, D.; Fedutik, Y.; Petrov, A. I.; Sukhorukov, G. B.; Mohwald, H. *Colloids Surf.* **2003**, *224*, 175–183.
(48) Antipov, A. A.; Sukhorukov, G. B. *Adv. Colloid Interface Sci.* **2004**, *111*, 49–61.
(49) De Geest, B. G.; Sanders, N. N.; Sukhorukov, G. B.; Demeester, J.; De Smedt, S. C. *Chem. Soc. Rev.* **2007**, *36*, 636–649.
(50) Zhu, H.; Stein, E. W.; Lu, Z.; Lvov, Y. M.; McShane, M. J. *Chem. Mater.* **2005**, *17*, 2323–2328.
(51) In the earlier study the minimum inhibitory concentration (MIC) for polymer **5** was not determined against *P. aeruginosa*. However, in more recent work, we determined the MIC for **5** vs *E. coli* (D21 mutant strain, incubation in the dark for 12 h) as 0.3 μg/mL.
(52) Ding, L. P.; Chi, E. Y.; Chemburu, S.; Ji, E.; Schanze, K. S.; Lopez, G. P.; Whitten, D. G. *Langmuir* **2009**, *25*, 13742–13751.
(53) Ding, L. P.; Chi, E. Y.; Schanze, K. S.; Lopez, G. P.; Whitten, D. G. *Langmuir* **2010**, *26*, 5544–5550.
(54) Epand, R. M.; Epand, R. F. *Biochim. Biophys. Acta, Biomembr.* **2009**, *1788*, 289–294.
(55) Corbitt, T. S.; Zhou, Z. J.; Tang, Y. L.; Graves, S.; Whitten, D. G. *ACS Appl. Mater. Interfaces* **2011**, web ASAP, DOI: 10.1021/am200277c.
(56) Wang, Y.; Tang, Y. L.; Zhou, Z. J.; Ji, E.; Lopez, G. P.; Chi, E. Y.; Schanze, K. S.; Whitten, D. G. *Langmuir* **2010**, *26*, 12509–12514.